Check for updates

Polymer Engineering & Science

WILEY | spe INSPIRING PLASTICS PROFESSIONALS

RESEARCH ARTICLE OPEN ACCESS

Recyclability of Polystyrene Bead Foams: Degradation Behavior over 10 Extrusion Cycles

Christian Töpfer[1] | Kristina Schüllner[2] | Holger Ruckdäschel[1,2]

[1]Polymer Engineering Department, University Bayreuth, Bayreuth, Germany | [2]Neue Materialien Bayreuth GmbH, Bayreuth, Germany

Correspondence: Christian Töpfer (christian.toepfer@uni-bayreuth.de)

Received: 2 October 2025 | **Revised:** 24 November 2025 | **Accepted:** 1 December 2025

Keywords: bead foam | degradation | extrusion | foaming | particle foam | polystyrene | recycling

ABSTRACT

This study investigates the recyclability of expandable polystyrene (EPS) bead foams under conditions aligned with the EU Packaging and Packaging Waste Regulation (PPWR) by simulating 10 consecutive extrusion cycles with a consistent 35 wt% recycled fraction. Although molar mass distribution and MFI remained nearly constant across all cycles, mechanical properties deteriorated during the first four cycles. Compression modulus decreased by 24%, flexural modulus by 14% and flexural strength by 21% in these initial cycles. Faster pentane diffusion, reflected in shorter steaming times, indicates that changes in diffusion behavior, rather than chain scission, govern the loss in mechanical performance. After Cycle 4, both processing behavior and mechanical properties reached a plateau, demonstrating that the required 35 wt% recycled content leads to a stable material condition for future industrial practice. A complete post-use recycling loop (C + 1), including prefoaming, welding, compression, shredding, and pelletizing, revealed the strongest degradation, with a 15% drop in molar mass and an increase in MFI, which was caused primarily by the pelletizing step. Overall, the results show that EPS bead foams can withstand multiple recycling cycles when blended with virgin material, while highlighting that pelletizing and blowing agent diffusion must be monitored closely in circular EPS production.

1 | Introduction

Polystyrene (PS) is one of the most widely used polymers in industry due to its low cost, rigidity, and ease of processing. It plays a significant role in the foaming industry, especially due to its excellent insulation properties. EPS is commonly found in single-use food packaging such as cups and trays, as well as in general packaging applications [1–3]. Additionally, modified forms like high-impact Polystyrene (HIPS) are important in the electronics and housing sectors due to their enhanced toughness [4].

Despite its widespread use and various benefits of its applications, environmental concerns about polystyrene have been growing in recent years. As for other large volume polymers, its persistence in the environment and low recycling rates have been reviewed critically [5, 6]. Therefore, understanding the challenges of PS recycling and evaluating its long-term recyclability are essential to assess its potential for multiple recycling cycles and identify its limitations.

Recycling methods are generally categorized into material and chemical recycling [7].

For PS, pyrolysis is considered one of the most effective chemical recycling methods, offering high yields [8] but at the cost of high energy consumption [9, 10]. This process involves heating the material in an oxygen-free environment at temperatures around

This is an open access article under the terms of the Creative Commons Attribution License, which permits use, distribution and reproduction in any medium, provided the original work is properly cited.

© 2025 The Author(s). *Polymer Engineering & Science* published by Wiley Periodicals LLC on behalf of Society of Plastics Engineers.

Highlights

- PS bead foams recycled up to 10 extrusion cycles were investigated.
- Minor degradation occurred, plateauing after four cycles.
- 65% virgin PS stabilized processing and foam properties.
- Pelletizing caused the strongest degradation in closed-loop recycling.
- Steaming time correlates with mechanical properties of PS-foam.

350°C–600°C, resulting primarily in the recovery of styrene monomers. These monomers can then be purified through processes such as distillation [11, 12].

Laboratory studies have demonstrated styrene monomer recovery rates of up to 99% via pyrolysis under controlled conditions [11, 13–16]. However, scaling this process for industrial use remains a challenge. Reed et al. [17] proposed a potential setup involving a pyrolysis reactor, followed by a heat exchanger and two distillation columns. Their analysis indicated that, assuming a pyrolysis efficiency of 0.6, the total theoretical energy demand could be as low as ≤10 MJ/kg for monomer recovery [17]. First industrial-scale chemical recycling of PS has been implemented by companies such as Indaver and Agilyx, with plants designed to process multiple tons of PS per day and recover styrene monomer for reuse [18, 19].

In contrast to chemical recycling routes, mechanical recycling is already well established in the polystyrene industry. It involves reprocessing post-consumer or post-industrial PS waste without altering its chemical structure. The typical mechanical recycling workflow includes separation of different polymers, washing and grinding, followed by reprocessing into pellets or granulate [20].

While more accessible, mechanical recycling often leads to material degradation over multiple cycles, limiting its long-term performance. To achieve high-quality output, recycled PS is typically blended with virgin material. Many challenges in PS recycling are not primarily technical but rooted within economic, logistical, and contamination-related problems [5].

However, in practice, EPS impresses with a noteworthy recycling rate across the globe. EPS protective and insulated packaging is reported to be recycled at scale in more than 38 countries, resulting in a recycling rate of above 30 wt% [21]. Recent reports by Conversio [22] and the European Commission's Joint Research Centre (JRC) [23] highlight the remarkable progress achieved in the recycling of PS and EPS in recent years. In Europe, for example, a recycling rate of roughly 40% is already achieved, and the numbers are steadily increasing [22]. These unique achievements have recently been recognized by the United Nations Environment Programme (UNEP) in their recent report "Plastic Pollution Science" [24] stating EPS transport packaging (the biggest EPS packing application) as one of only six packaging formats worldwide to be recycled at a bigger scale.

Despite these advances, EPS recycling is still limited by logistical and economic barriers, primarily caused by the extremely low density of post-consumer EPS. The high volume-to-weight ratio of uncompacted EPS makes collection and transport inefficient and costly. However, Larrain et al. [25] showed that mechanical recycling of PS can already be profitable with an internal rate of return of 14%.

Another major barrier to higher recycling rates is contamination. Post-consumer PS from food packaging is often soiled with food residues, adhesives, and labels. These impurities reduce recyclate quality and restrict its use in high-value applications. Mechanically recycled PS cannot be reintroduced into food-grade packaging because typical post-consumer streams contain stabilizers, pigments, antistatic agents, glass fibers, and flame retardants that are not suitable for food contact [2, 26–30]. While food packaging is not the focus of this study, these restrictions illustrate the challenges faced by PS recycling.

Even for non-food applications, mechanical recycling still suffers from an inherent limitation: a progressive degradation of the material within each reprocessing cycle [10]. The combination of high heat and intense mechanical shear stress during extrusion alters the polymer's molecular structure, leading to downcycling [31].

Thermal degradation mechanisms of PS in the absence of oxygen require high temperatures. Degradation typically starts at temperatures of around 275°C–350°C in inert conditions [32, 33]. Cameron et al. [34] reported minor molar mass changes below 300°C while significant volatilization occurred at higher temperatures (>300°C). The specific degradation pathway and its kinetics are significantly influenced by the polymer's synthesis method [34], molar mass (M_w) [32] and in the case of high-impact PS (HIPS), the presence of the polybutadiene (PB) phase [35]. Regarding the synthesis route, anionic PS is highly regular and therefore initially more stable in comparison to radical PS with a thermal initiation. Despite these initial differences, the degradation characteristics of both types become nearly identical after about 10% of the material has been converted to volatiles [34].

Additionally, higher M_w increases the rate of thermally induced random chain scission [32, 33]. Compared to degradation under inert conditions, thermo-oxidative degradation for HIPS has been observed at 90°C in a forced ventilation oven [35]. In contrast, oxygen-deficient atmospheres like during extrusion can tolerate temperatures up to 200°C without noticeable material degradation [35].

Extrusion is a primary cause of material degradation during the mechanical recycling of PS, as the process simultaneously exposes the polymer to high thermal and mechanical stresses [36]. This combined loading leads to chain scission and a decrease in M_w [36, 37] and viscosity [37, 38]. The degradation mechanism during extrusion is synergistic. Mechanical shear can effectively lower the temperature required for thermal

15482634, 2026, 3, Downloaded from https://4spepublications.onlinelibrary.wiley.com/doi/10.1002/pen.70290 by Universitaet Bayreuth, Wiley Online Library on [07/04/2026]. See the Terms and Conditions (https://onlinelibrary.wiley.com/terms-and-conditions) on Wiley Online Library for rules of use; OA articles are governed by the applicable Creative Commons License

degradation. It has been shown that shear-induced degradation of PS can happen 50°C below the initiation of purely thermal degradation mechanisms [38]. For this reason, static thermal stability tests are often misleading and cannot accurately predict a polymer's stability during processing [37, 38]. Springer et al. [37] observed an 18% decrease in M_w after five extrusion cycles and found that higher screw speeds caused a greater reduction. In contrast, Capone et al. [39] concluded that faster screw speeds result in smaller reductions of M_w. They addressed these results with a shorter residence time in the extruder and potential wall-slip phenomena that reduced the actual shear stress applied to the polymer. Remili et al. observed a continuous degradation over eight extrusion cycles for PS resulting in a drop in modulus and molar mass [40]. For HIPS, degradation initiates at the more sensitive PB rubber phase [2, 36, 41, 42]. In a study by Velásquez et al. [2] yogurt cups were subjected to 10 cycles of repeated extrusion. The results showed a significant loss of impact strength and rigidity as the PB phase degrades through chain scission, oxidation, and crosslinking. Similar findings were reported in other studies [41–44]. Overall, the material exhibited a 41% increase in MFI and a 28% decrease in impact strength [2].

Managing degradation during melt extrusion is therefore critical for both HIPS and standard PS (GPPS). This is particularly important because recycling economics are already constrained by high processing costs and limited material profitability.

The influence of repeated mechanical recycling on bead foaming behavior and the resulting foam properties has not yet been systematically investigated. To reflect industrial practice, this study incorporates virgin PS to partially compensate for degradation effects during repeated processing. This topic is of particular relevance, as the experimental design follows the principles outlined in the EU Packaging and Packaging Waste Regulation (PPWR 2025/40), which mandates a minimum recycled content of 35 wt% for non-food contact packaging [45]. Therefore, the aim of this research is to evaluate the degradation behavior of EPS bead foams over 10 extrusion cycles, to determine how repeated mechanical recycling influences molar mass, processing behavior, and foam properties to identify the critical processing steps that drive material degradation.

2 | Materials and Methods

2.1 | Materials

Virgin polystyrene (PS) Edistir N 3380 used as base polymer was supplied by Versalis S.p.A. (San Donato Milanese, Italy).

A nucleating agent (NA) (polyethylene wax, melting range 121°C–127°C) and a coating additive (CA) consisting of a mixture of 60 wt% glyceryl tristearate, 30 wt% glyceryl monostearate, and 10 wt% zinc stearate were obtained from BASF SE (Ludwigshafen, Germany).

Isopentane (purity ≥ 99%) and n-pentane (purity ≥ 95%) were purchased from Carl Roth GmbH + Co. KG (Karlsruhe, Germany).

The blowing agent mixture consisted of n-pentane and isopentane in a weight ratio of 80:20 (n/iso). The recycling content per extrusion cycle was set to 35 wt% recycled material blended with 65 wt% virgin PS.

To ensure comparability with industrial process quality, K-510e virgin EPS was supplied by BEWI ASA (Trondheim, Norway) as industrial benchmark material.

2.2 | Study Design

In total, 10 extrusion cycles were performed to evaluate the cumulative effects of repeated mechanical recycling.

In each cycle, two types of material were produced: unloaded material for reprocessing and pentane-loaded microgranulate for foaming. NA was added to all materials, but only the material intended for foaming was loaded with 6 wt% of the n-/isopentane mixture and coated with 0.3 wt% of the CA.

After each cycle, 35 wt% of the produced unloaded material was mixed with 65 wt% of virgin PS to prepare material for the next extrusion step. The first cycle started with 100 wt% virgin material. This approach replicates current industrial recycling practice and reflects the guidelines outlined in the European Union Packaging and Packaging Waste Regulation for 2030 [45], which promotes continuous usage of recycled content.

This method allows the gradual build-up of the recycled fraction of multiple recycling runs under realistic processing conditions, allowing the degradation behavior to be monitored across multiple extrusion and foaming steps.

Additionally, one complete recycling loop, including bead foaming, welding, compression, shredding and pelletizing, was performed, comparable to a full EPS life cycle from production to reuse in the non-food-contact packaging industry. This loop is referred to as cycle C + 1 and was carried out to ensure that material degradation occurs primarily during the extrusion of microgranulate. A full illustration of the trial plan is shown in Figure 1, further information can be found in the Supporting Information.

2.3 | Processing

2.3.1 | Extrusion Process

Prior to extrusion, all PS granulates were dried for at least 12 h at 50°C. Microgranulates were manufactured using a Reifenhäuser tandem foam extrusion line (Troisdorf, Germany) combined with an underwater granulator (UWG) from Econ (Steyr-Gleink, Austria). The tandem line consisted of a twin-screw extruder (A-Extruder, $D = 41$ mm, $L/D = 43$) and a downstream single-screw extruder (B-Extruder, $D = 50$ mm, $L/D = 30$). The UWG was equipped with a rotating knife featuring 8 blades, operated at 2000 rpm.

The pentane mixture was dosed into the twin-screw extruder using an Ecofoam dosing system (LEWA GmbH, Leonberg,

15482634, 2026, 3, Downloaded from https://4spepublications.onlinelibrary.wiley.com/doi/10.1002/pen.70290 by Universitaet Bayreuth, Wiley Online Library on [07/04/2026]. See the Terms and Conditions (https://onlinelibrary.wiley.com/terms-and-conditions) on Wiley Online Library for rules of use; OA articles are governed by the applicable Creative Commons License

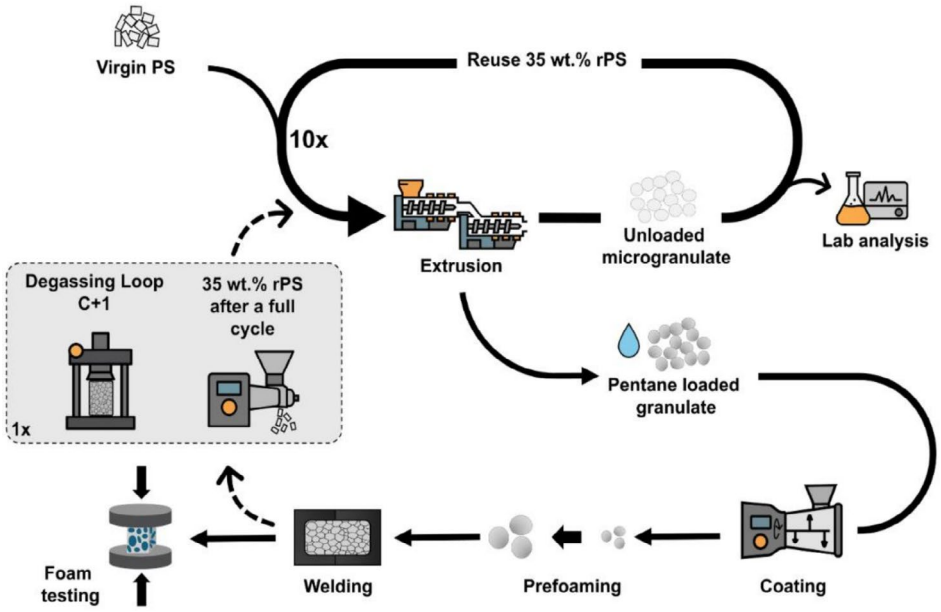

FIGURE 1 | Schematic illustration of the 10-cycle mechanical recycling process including extrusion, foaming, welding, and testing, and the additional closed-loop EPS recycling (Cycle C + 1).

Germany). The blowing agent was introduced into the molten PS in the A-Extruder, which operated at 80 rpm, at a temperature between 210°C and 230°C for all cycles.

The resulting one-phase mixture was transferred to the single-screw extruder, operated at 27 rpm, and cooled to 210°C before getting transferred into the melt pump and die plate. The die plate consisted of five nests, each equipped with 5 × 0.8 mm die holes, designed to produce microgranulate. The die plate temperature was maintained at higher temperatures (270°C for unloaded and 290°C for pentane loaded granules) to prevent premature solidification. Water temperatures and pressure during underwater granulation were 30°C–34°C and 6 bars. A constant throughput of 20 kg/h was maintained.

2.3.2 | Bead Foaming and Part Fabrication

Prior to prefoaming, the pentane-loaded granulate was coated with 0.3 wt% CA to improve bead surface quality and processing stability. Batches of 4 kg were coated at room temperature using a Type 10 Ploughshare laboratory mixer from Lödige Process Technology (Paderborn, Germany). The mixer operated at 200 rpm for 100 s to ensure a uniform distribution of the coating agent on the granulate surface.

Steam-based prefoaming was carried out using the X-Line 3 system from Kurtz Ersa (Kreuzwertheim-Wiebelbach, Germany). The prefoaming process continued until a sensor detected a target volume of 65 L, corresponding to a bulk density of 19 g/L (±1 g/L). The initial mass was 1240 g of loaded granulate. The steam/air mixture was set to 100% steam, the mixer operated at 50 rpm, steam pre-pressure was maintained at 0.7 bar and steam vessel pressure at 0.5 bar. This approach leads to variations in steaming times at constant steaming pressure, while ensuring consistent bulk density throughout all cycles. To monitor the prefoaming process, bulk density was measured both before and after steaming to confirm that target density had been reached and to evaluate the consistency of the process. The prefoamed beads were conditioned at room temperature for 24 h prior to molding.

Steam-chest molding was conducted using the TransTec 72/52 PP system by Teubert Maschinenbau GmbH (Blumberg, Germany). The fixed parameters included a mold geometry (rectangular plate) of 200 × 290 × 20 mm^3 and the use of four fillers placed in each corner of the mold. The steaming process consisted of two cross-steam phases at 1.2 bar for 5 s each, followed by autoclave steaming at 1.4 bar for 3 s. Cooling was conducted up to 70°C, and the demolding foam pressure was maintained at 0.3 bar. The target density of the molded part was 20 g/L (±1 g/L). To maintain uniform part density, the silo pressure was continuously adjusted.

2.3.3 | Recycling Process (Closed-Loop Simulation)

The recycling cycle C + 1 simulates a complete material lifetime up to the point of recycling. It consists of five key stages:

1. Prefoaming: The material is expanded to achieve a bulk density of 19 g/L.
2. Welding: The parts are welded, resulting in a part density of about 22 g/L.
3. Compressing: The welded components are compacted to prepare them for further processing.
4. Shredding: The compressed material is shredded, increasing the bulk density to around 60 g/L.
5. Pelletizing: The shredded material is transformed into pellets with a final bulk density of approximately 500 g/L.

The prefoaming process is performed using the X-Line 3 machine from Kurtz Holding GmbH (Kreuzwertheim, Germany).

15482634, 2026, 3, Downloaded from https://4spepublications.onlinelibrary.wiley.com/doi/10.1002/pen.70290 by Universitaet Bayreuth, Wiley Online Library on [07/04/2026]. See the Terms and Conditions (https://onlinelibrary.wiley.com/terms-and-conditions) on Wiley Online Library for rules of use; OA articles are governed by the applicable Creative Commons License

Welding is handled by the TVZ 162/100 PP unit from Teubert Maschinenbau GmbH (Blumberg, Germany) and a tool with a dimension of $1000 \times 600 \times 90\,mm^3$. Compression is achieved with a 600-ton press manufactured by WICKERT Maschinenbau GmbH (Landau, Germany). The shredding step utilizes a cutting mill from Wanner Technik GmbH (Wertheim, Germany), and the final pelletizing is completed using a pelletizing unit from Amandus Kahl GmbH & Co. KG (Reinbek, Germany). This step was performed with a die plate featuring 8 mm perforations and a thickness of 24 mm, at a rotational speed of about 90 rpm (utilization of 75%). This process is designed to simulate one full "material lifetime" before reprocessing.

2.4 | Characterization Methods

Gel permeation chromatography (GPC) measurements in chloroform ($CHCl_3$) were carried out using an instrument equipped with a linear XL SDV gel column (particle size = 5 μm) with a separation range of 100–3,000,000 Da (PSS, Mainz, Germany). A refractive index detector (1200 Series, Agilent Technologies) was used for detection. HPLC-grade $CHCl_3$ was used as both the solvent to dissolve the polymer and the eluent. Measurements were performed at a flow rate of 0.5 mL/min at room temperature. HPLC-grade toluene was used as the internal standard. Calibration was performed using a narrowly distributed polystyrene (PS) homopolymer from a PSS calibration kit. An injection volume of 20 μL was used. Before analysis, the sample was dissolved in $CHCl_3$ and filtered through a 0.22 μm PTFE filter to remove the insoluble NA from the PS sample.

The melt volume index (MVI) represents the rate at which a molten polymer is extruded through a standardized die with a specific length of 8 mm and a diameter of 2.095 mm following EN ISO 1133 standards. During testing, the extruded volume per unit time is measured. MVI measurements were performed using a MeltFlow@on device (KARG Industrietechnik GmbH, Illertissen, Germany) operated under a testing load of 5 kg at 200°C. At least 20 measurement points were recorded for each material cycle C1-10 and C + 1. For all materials, mean values of MVI were determined and melt flow index (MFI) value was calculated based on Equation (1). The melt density ρ_{melt} of 0.97 g/cm^3 at 200°C was used for PS, as reported by the manufacturer.

$$MFI = \frac{MVI}{\rho_{melt}} \tag{1}$$

The analytical work accompanying the prefoaming and welding includes the determination of blowing agent content at four distinct stages: before prefoaming, before welding, in the produced parts 5 days after production, and again 4 weeks after production. The determination of the blowing agent content was carried out using a gravimetric method. First, the empty sample containers were weighed. Then, the containers were weighed again after being filled with microgranulate or foamed beads. The filled containers were subsequently placed in an oven at 130°C for 1 h to allow the blowing agent to evaporate. After the heating step, the containers with the remaining beads were weighed once more. The pentane content was then calculated based on the weight loss observed during the heating process.

All mechanical test specimens were conditioned for at least 48 h in a standard atmosphere prior to testing. Compression testing was done according to ISO 844. For each recycling cycle, at least five specimens were tested. The samples were tested including the intact foam skin at the top and bottom surface. All specimens were square-shaped (2500 mm^2) with a thickness of 20 mm. Testing was performed using a Z050 universal testing machine (ZwickRoell GmbH & Co. KG, Ulm, Germany). For data evaluation a custom Python script was used to calculate the elastic modulus. This approach was chosen to reduce potential human error during data extraction and analysis, as described by Albuquerque et al. [46].

Three-point bending (3-PB) tests were performed on a ZwickRoell Z2.5 based on ISO 1209-1. All samples included the original, untrimmed foam skins (dense outer layer) on both the compression and tension sides of the test specimen.

The test specimens had a length of 120 ± 1.2 mm, width of 25 ± 0.25 mm and a thickness of 20 ± 0.2 mm. The span length between the supports was set to 100 mm. Due to the relatively short span length in relation to the sample thickness, pure bending conditions were not achieved. As a result, the measured mechanical response represents a combination of multiple deformation modes, such as bending shear and compression. Therefore, all three-point bending results are only comparable within this study and should not be interpreted as absolute flexural properties.

Additionally, all mechanical results were normalized (E_{norm} and σ_{norm}) to a reference density ρ_{target} of 20 kg/m^3, as the measured densities $\rho_{measured}$ across different cycles ranged between 21.6 and 22.8 kg/m^3. Normalization was performed using Equations (2) and (3) [47], based on the measured values for both modulus $E_{mearsured}$, flexural and compression strength ($\sigma_{measured}$), the corresponding densities.

$$\sigma_{norm} = \sigma_{measured}\left(\frac{\rho_{target}}{\rho_{measured}}\right)^n \tag{2}$$

$$E_{norm} = E_{measured}\left(\frac{\rho_{target}}{\rho_{measured}}\right)^n \tag{3}$$

Following the approach described by Gibson and Ashby [47], an exponent factor of $n = 2$ was applied for elastic material behavior (e.g., elastic modulus), while $n = 1.5$ was used in cases dominated by plastic yielding or brittle fracture (flexural and compression strength values). This allowed for a consistent comparison of mechanical properties across samples with slightly varying densities.

3 | Results and Discussion

3.1 | Process Stability and Material Degradation

Process stability in extrusion was unaffected across all cycles without pentane loading. However, the addition of pentane significantly lowered the melt viscosity, resulting in a

15482634, 2026, 3, Downloaded from https://4spepublications.onlinelibrary.wiley.com/doi/10.1002/pen.70290 by Universitaet Bayreuth, Wiley Online Library on [07/04/2026]. See the Terms and Conditions (https://onlinelibrary.wiley.com/terms-and-conditions) on Wiley Online Library for rules of use; OA articles are governed by the applicable Creative Commons License

pressure decrease of approximately 30 bars at the die plate. The reduced melt strength due to the plasticizing effect of pentane [48–50], affected stable processing. To counteract these effects, adjustments to the die plate temperature were necessary between the unloaded (270°C) and the pentane loaded granulates ($T_{\text{die plate}} = 290°C$) to achieve stable extrusion behavior. These updated parameters were kept constant over all 10 extrusion runs. Only the knife speed of the pelletizer was occasionally adapted from 2000 rpm to a max of 2700 rpm in cases where partial die hole blockage appeared. This adjustment was crucial to maintain near constant bead sizes and to minimize the effect of bead size variation on mechanical properties as macro-porosity due to bigger bead sizes provoke crack initiation [51].

In comparison to C1–C10, which maintained die pressures at 50–60 bar, the full degassing step C + 1 showed further reduction to approximately 40 bar. These observations indicate a further reduction in melt viscosity caused by thermomechanical degradation during the recycling process.

The prefoaming process resulted in highly homogeneous bulk densities across all recycling cycles, consistently achieving the target bulk density of 19 ± 1 g/L. To achieve consistent bulk densities, the required steaming time was automatically adjusted depending on the material condition in each cycle. This regulation was based on two fixed parameters: the weighed-in material quantity and a sensor to reach a volume of 65 L. The steaming process continued until the foam reached this specified volume, allowing the system to dynamically adapt the steaming time to the material's foaming behavior.

Across cycles 1 to 10, a high level of consistency and reproducibility was observed. Only the reference material (K510e) and C + 1 deviated from this trend, exhibiting shorter steaming times due to differences in molar mass. The reduced viscosity resulted in faster expansion and shorter steaming time in prefoaming.

Consistent welding quality in steam-based molding process was achieved across all recycling cycles without modifying the steaming parameters. For evaluation, the density of each molded part was determined, and the welding quality was assessed by optical analysis of the fractured parts to verify whether the welding was sufficient to produce intrabead failure. To maintain a uniform part density of 22 ± 1 g/L, filling parameters—specifically filling time (3–6 s) and silo pressure (0.1–0.6 bar) – were continuously adjusted. This demonstrates the sensitivity of the process to material conditions.

Cycle time, as the most dominant factor influencing economic viability, was primarily governed by foam pressure reduction within the mold prior to demolding. Demolding was only feasible after cooling to 70°C and a sufficient drop in pressure of the beads against the inner wall of the mold (to 0.3 bar, value obtained from preliminary tests) to ensure dimensional stability. The duration of pressure release was influenced, that is, by the residual content of the blowing agent and its retention time within the polymer matrix (Figure 4), which is governed by the material's diffusivity. This stabilization period constitutes the primary factor determining the overall cycle time.

Reproducibility was confirmed for all materials, with standard deviations in part density remaining below 0.35 g/L. This indicates a stable and controlled process window, provided that dynamic adjustments to filling conditions are implemented.

These findings underscore the importance of dynamic process control in industrial applications, where economic viability is closely tied to cycle time and consistent product quality. The following diagram (Figure 2) illustrates the cycle times (in seconds) for various molding cycles, ranging from the reference material K-510e through Cycle +1 and Cycles 1 to 10:

From Cycle 1 to Cycle 3, a reduction in cycle time is observed. This trend is attributed to decreasing stabilization times, which are influenced by a progressive reduction in residual blowing agent content and its retention time within the polymer matrix. The increased diffusivity of the blowing agent may be related to morphological changes, such as a redistribution of polymer from cell walls to struts, leading to thinner walls, higher effective porosity, and consequently faster pressure decay. As a result, internal foam pressure dissipated more rapidly, enabling earlier demolding and thus shorter cycle times.

From Cycle 3 to Cycle 10, the cycle time plateaus, indicating that the stabilization behavior of the material reaches a steady state. This suggests that the residual blowing agent content, and its retention characteristics stabilize after several recycling loops, leading to consistent demolding conditions due to similar material formulation.

In comparison, the reference material (K-510e) exhibits a significantly longer cycle time. This is due to higher stabilization requirements. This material requires more time for internal pressure to drop to the demolding pressure (0.3 bar).

Cycle +1 (full lifetime loop) shows a similar cycle time to cycles 4–10. This result indicates that the material reaches stable

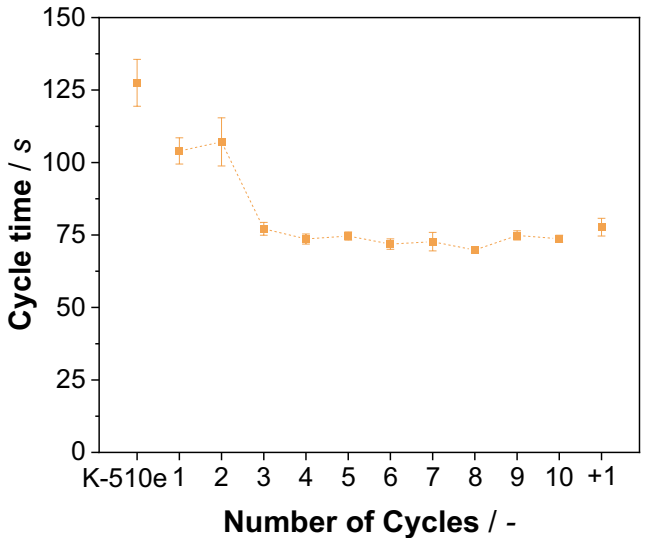

FIGURE 2 | Cycle time during steam-based molding, including cycles 1–10, benchmark virgin EPS K-510e, and the complete loop C + 1. The dotted line is included as a visual guide to indicate trends between the cycles.

15482634, 2026, 3, Downloaded from https://4spepublications.onlinelibrary.wiley.com/doi/10.1002/pen.70290 by Universitaet Bayreuth, Wiley Online Library on [07/04/2026]. See the Terms and Conditions (https://onlinelibrary.wiley.com/terms-and-conditions) on Wiley Online Library for rules of use; OA articles are governed by the applicable Creative Commons License

processing behavior after several recycling steps. This suggests that even after a complete recycling loop, the material retains consistent foaming and demolding characteristics. Such stability is essential for industrial applications, as it enables predictable cycle times, supports dynamic process control, and ensures economic viability in serial production.

3.2 | Molecular Degradation and Pentane Retention

The MFI exhibited a gradual decrease over the 10 cycles (Figure 3), which does not align with the assumption of decreasing melt viscosity due to thermal and thermomechanical degradation during repeated extrusion. However, when considering values C1–C10, which range between 2.9 and 3.4 g/10 min, it becomes evident that the variation is minimal. Notably, the change in MFI between virgin (N 3380) and once-processed material (C1) is approximately two times as large as the total variation through all 10 extrusion cycles.

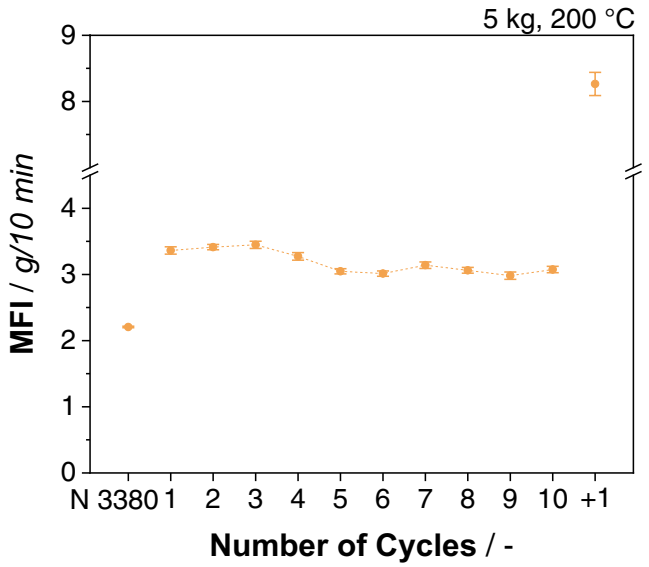

FIGURE 3 | Melt flow index measurements at 200°C and 5 kg weight, including all cycles, unprocessed base material, and degassing cycle C + 1. The dotted line is included as a visual guide to indicate trends between the cycles.

This suggests that the addition of 65% neat material effectively stabilizes the melt properties and mitigates the accumulation of degradation effects over multiple extrusion steps. The relatively constant MFI values imply that under these extrusion conditions, the cumulative degradation per cycle is minor and fully compensated by the virgin fraction.

In contrast, the fully recycled and degassed sample (C + 1) exhibits a substantial increase in MFI to 8.0 ± 0.2 g/10 min. This rise indicates a significant reduction in melt viscosity due to extensive chain scission and M_w reduction during degassing cycle. Further information regarding the degassing cycle (C + 1) can be found under Section 3.4.

To relate changes of MFI with the M_w changes GPC analysis was performed. Figure 4 shows the results of GPC. M_w was nearly constant (C1–C10) while a significant drop was observed by Cycle C + 1. Dispersity $Đ$ was measured between 2.0 and 2.4 for all cycles after reprocessing, including C + 1. Since GPC traces show no significant broadening and $Đ$ remains nearly stable while M_w decreases in C + 1, these results indicate a uniform, randomly distributed chain scission mechanism affecting the entire molar mass distribution, rather than targeting high molecular weight fraction.

The variation in blowing agent content across multiple stages of the bead foaming process over all 10 cycles, including C + 1 and the reference cycle labeled K-510e is shown in Figure 5.

Four stages of the bead foaming process are represented: loaded microgranules immediately before prefoaming, expanded beads directly before welding, molded parts after 5 days, and molded parts after 4 weeks.

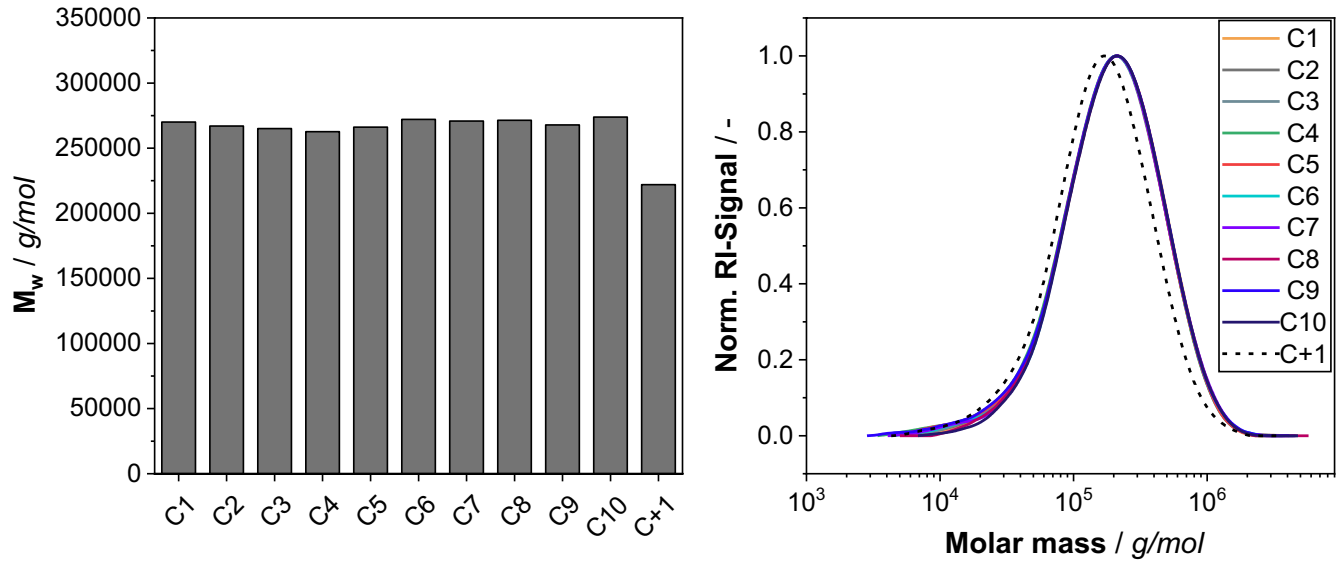

FIGURE 4 | Molar mass changes over all extrusion cycles measured via GPC (left), normalized RI signal (right).

15482634, 2026, 3, Downloaded from https://4spublications.onlinelibrary.wiley.com/doi/10.1002/pen.70290 by Universitaet Bayreuth, Wiley Online Library on [07/04/2026]. See the Terms and Conditions (https://onlinelibrary.wiley.com/terms-and-conditions) on Wiley Online Library for rules of use; OA articles are governed by the applicable Creative Commons License

The data reveal a marked decrease in blowing agent content in the molded parts from Cycle 1 through Cycle 4. Beyond the fourth cycle, the values stabilize, indicating a plateau in the degassing behavior of the blowing agent. Notably, the first cycle and K-510e exhibit comparable levels of blowing agents. C + 1 shows similar results to cycles 4–10.

The stabilization observed after several cycles may reflect an equilibrium state in the material system, which is critical for ensuring consistent part quality and performance in serial production. Parts made of EPS are often stored for a certain period after production to allow the residual blowing agent to evaporate from the molded part. The diagram shows that this removal time gets shorter from cycles 1 to 4, as there is already less residual blowing agent in the molded part after production. This trend may be related to morphological changes that also govern cycle times of welding, as pentane retention exhibits the same tendency as observed for cycle time in Figure 2.

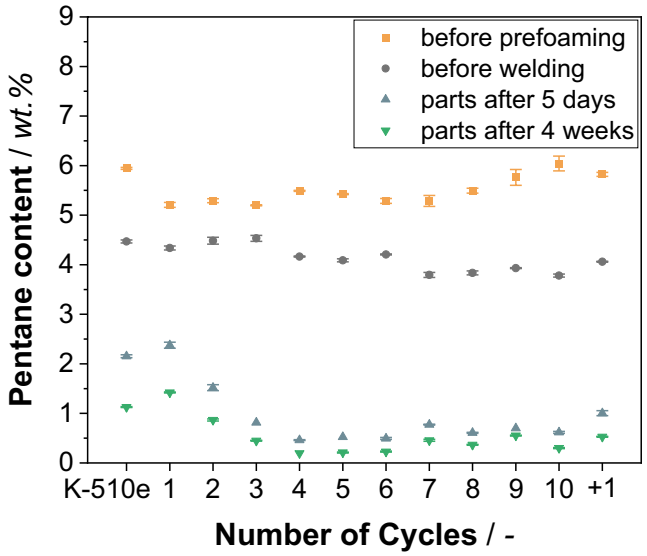

FIGURE 5 | Residual pentane content measured at different stages after processing. Values represent the average pentane content at each time point.

3.3 | Mechanical Performance of Recycled Bead Foams

The mechanical data illustrates the changes in static mechanical properties across all cycles (Figure 6). For comparison to industrial standards virgin PS (K-510e) was added to the data. All curves are normalized to a density of 20 kg/m^3 as described above. Cycle 1 performs comparable to K-510e in terms of compression strength at different compression levels, however, elastic modulus was found to be lower for K-510e. A progressive decrease in both compression modulus and compressive stresses at different strain values were observed with an increasing number of extrusions. This trend reflects a loss of stiffness and load-bearing capacity. The drop in compression is observed for all levels (10%, 25%, and 50%), however, the effect is strong at the first 4 runs and nearly constant for the extrusion cycles 5–10. From Cycle 5 onward, the measured values approach a plateau, which closely matches values obtained for the degassing cycle C + 1. These results indicate that a full recycling/degassing loop affects the mechanical performance as strongly as multiple extrusion cycles, considering the applied recycling rates. As shown in Figure 4, a distinct shift in molar mass distribution was only observed for the C + 1 sample. This leads to an increased diffusivity of the blowing agent and a drop in mechanical performance. The reduced barrier properties accelerate the loss of blowing agent during molding, resulting in shorter welding times (Figure 2). In contrast, the molar mass distribution did not shift after multiple extrusion cycles, however the welding times were still reduced, which could be linked to enhanced blowing agent diffusion. This assumption is supported by the residual pentane contents before and after welding (Figure 5). In Cycle 1, the total pentane content decreased by 44% during welding processes and 5 days of conditioning at room temperature (from 4.3 to 2.4 wt%), whereas in Cycle 10 the reduction reached 84% (from 3.8 to 0.6 wt%). The accelerated diffusion observed in later

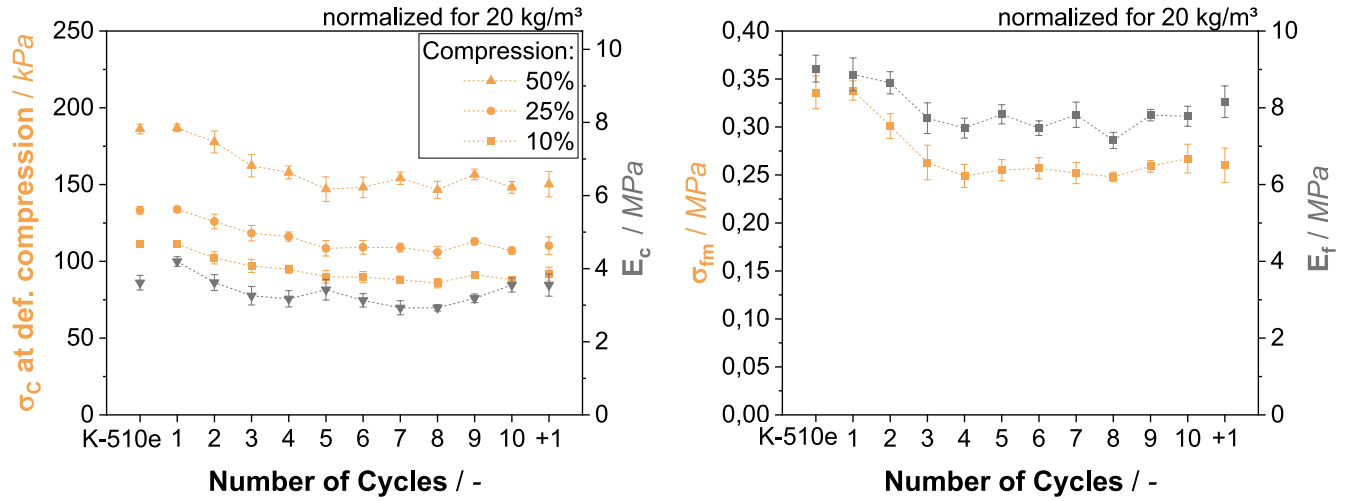

FIGURE 6 | Mechanical performance of all tested materials compared to the benchmark K-510e under compression (left) and three-point bending tests (right). The dotted line is included as a visual guide to indicate trends between the cycles. Compressive stress was evaluated at 10%, 25%, and 50% deformation.

15482634, 2026, 3, Downloaded from https://4spublications.onlinelibrary.wiley.com/doi/10.1002/pen.70290 by Universitaet Bayreuth, Wiley Online Library on [07/04/2026]. See the Terms and Conditions (https://onlinelibrary.wiley.com/terms-and-conditions) on Wiley Online Library for rules of use; OA articles are governed by the applicable Creative Commons License

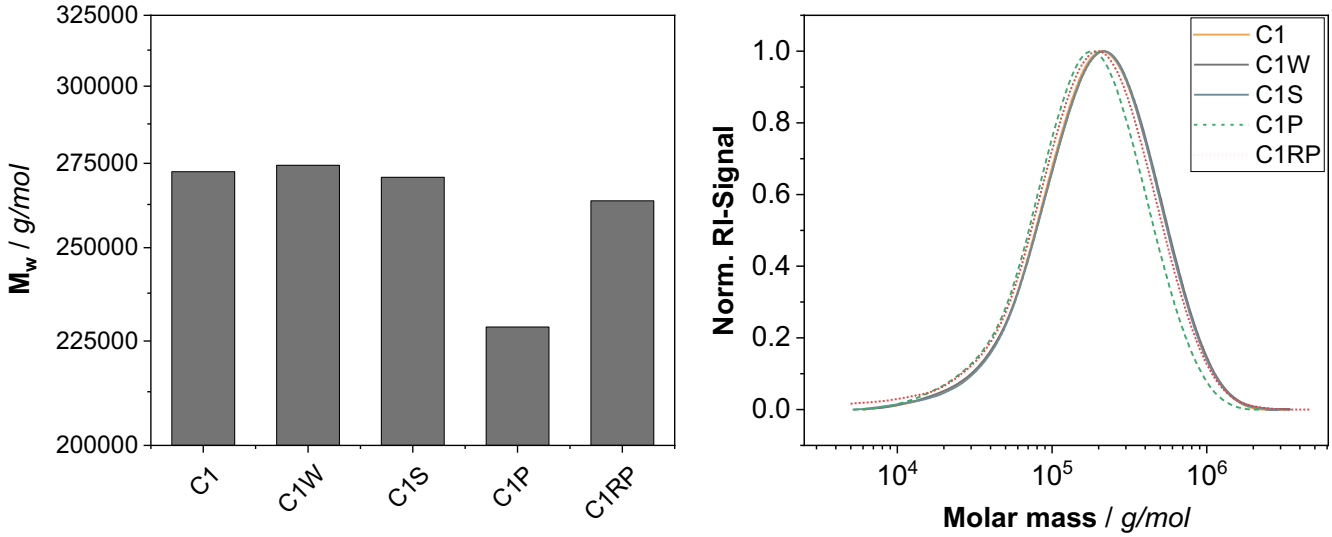

FIGURE 7 | Molar mass changes across the degassing cycle C + 1, including stages C1 processed, C1W welded, C1S shredded, C1P pelletized, C1RP reprocessed with 65% virgin material, measured via GPC (left: molar mass distribution; right: normalized RI-signal).

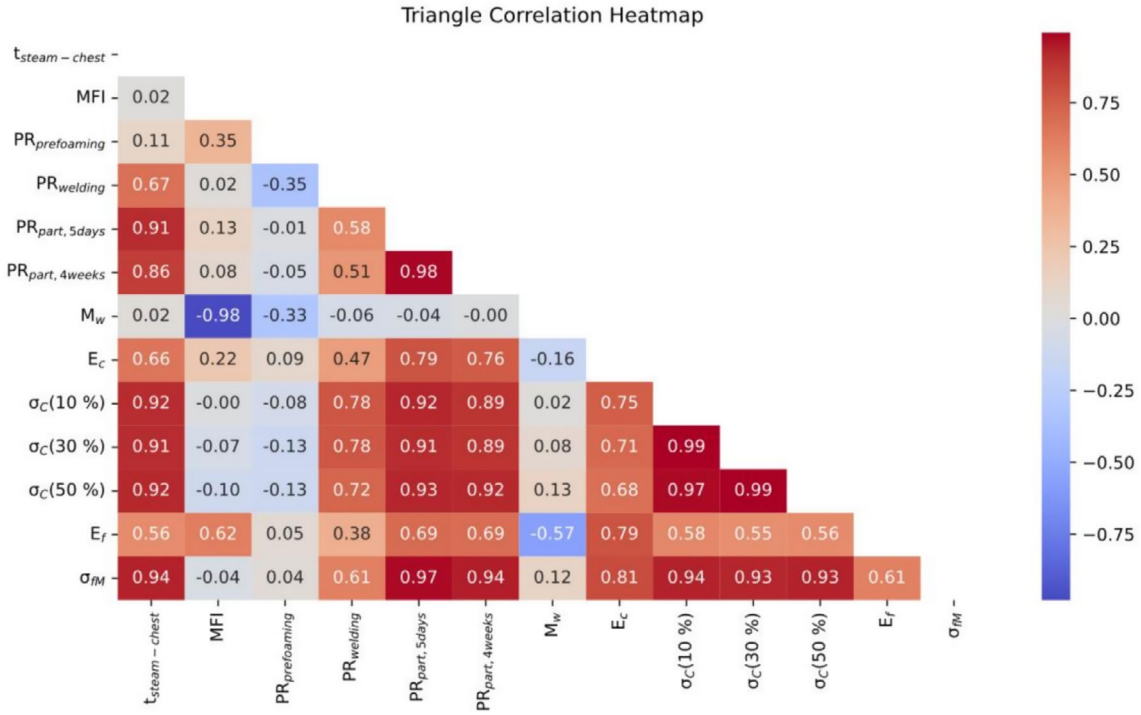

FIGURE 8 | Pearson's correlation coefficients matrix of processing parameters and material properties.

cycles likely reflects subtle morphological changes, potentially including thinner cell walls and thicker struts, that increase gas permeability.

The additional data gathered by 3-PB measurements supports these results (shown in Figure 5). All samples exhibited intrabead failure during three-point bending, confirming that bead welding was sufficient and that the observed mechanical changes are not related to insufficient fusion. While flexural properties of C1 are on the same level as industry standard (K-510e), flexural strength and modulus drop over the first 4 cycles by 21% in strength and 14% in modulus. These effects align with literature results of recycled materials [52, 53]. The observed changes in material behavior suggest that repeated processing cycles introduce additional macrostructural defects such as voids, or interfacial debonding. While these defects have only a minor impact on stiffness, they lead to internal stress concentrations that ultimately reduce the material's resistance to fracture.

3.4 | Closed-Loop Recycling Potential

As previous analysis suggested, the main degradation in this study was not only caused by multiple extrusion cycles but by the full degassing and recycling loop C + 1. Further analysis

15482634, 2026, 3, Downloaded from https://4spepublications.onlinelibrary.wiley.com/doi/10.1002/pen.70290 by Universitaet Bayreuth, Wiley Online Library on [07/04/2026]. See the Terms and Conditions (https://onlinelibrary.wiley.com/terms-and-conditions) on Wiley Online Library for rules of use; OA articles are governed by the applicable Creative Commons License

after all processing steps C1 after extrusion, C1W after welding, C1S after shredding, C1P after pelletizing and C1RP after another reprocessing step with 65% virgin material is shown in Figure 7. During prefoaming, welding, and shredding, only negligible changes in molar mass (M_w) are observed. In contrast, pelletizing causes a reduction in M_w of about 15%. Reprocessing can only partially compensate for this loss, leading to an increase of around 12%. Pelletizing was used solely to suit the pilot-scale equipment and is not necessarily standard industrial practice for this material. The extent to which pelletizing is applied in industry, and the associated shear intensity, remains unclear and may vary depending on process design. In our study, the intense shear forces involved in this step caused pronounced material degradation. Industrial pelletizing might be less shear-intensive or unnecessary as specific dosing units like Crammer Feeders [54] or Feed Enhancement Technology (FET) [55] can be used directly with shredded material. Alternatively, solvent-based hybrid methods for EPS recycling can be employed, in which volume reduction is achieved through dissolution [8, 56, 57], followed by mechanical recycling of the recovered polystyrene.

3.5 | Correlation Between Processing Parameters and Material Properties

To understand potential relationships between all measured processing parameters and material properties, a Pearson correlation analysis was performed using Python. While correlation does not imply causation, it can provide an indication of how strongly two variables co-vary. As expected, the analysis (Figure 8) reveals a strong negative correlation between the M_w and MFI ($R_p = -0.98$). However, no significant correlations were observed between compression mechanics and MFI/M_w. In contrast, the steaming time $t_{steam\text{-}chest}$ shows strong correlations with nearly all mechanical properties as well as with pentane retention behavior. This positive correlation can be explained by the fact that longer steaming time promotes stronger inter-bead welding, which not only enhances the mechanical integrity of EPS but also reduces pathways for pentane loss.

4 | Conclusions

This study assessed the recyclability of EPS bead foams under PPWR-relevant conditions by simulating 10 mechanical recycling cycles with a fixed 35 wt% recycled content. Although molar mass and MFI remained nearly constant across the 10 cycles, the mechanical properties nevertheless deteriorated during the first four cycles, indicating that factors other than chain scission contributed to the loss of performance. The compression modulus decreased by 24%, the flexural modulus by 14% and the flexural strength by 21%.

The faster pentane diffusion observed in later cycles, along with shorter steaming times, may indicate subtle morphological or macrostructural changes as main reason for reduced mechanical properties. To compensate for these changes, already a minor density increase of 3–4 kg/m^3 would effectively counteract the mechanical losses and result in partially recycled EPS foams with comparable mechanical properties and sufficiently low density.

After Cycle 4, the material properties reached a plateau, with mechanical performance remaining nearly constant up to Cycle 10 due to the dilution effect of the 35 wt% recycled fraction. This steady-state condition reflects the expected material response under future industrial recycling conditions defined by PPWR.

In contrast, the complete post-use recycling loop (C + 1) revealed significant degradation, including a substantial drop in molar mass of 15% and an increase in MFI to 8.0 ± 0.2 g/10 min, which was primarily induced during the pelletizing stage. These findings identify pelletizing as the most critical degradation point in the mechanical recycling chain. Mitigation strategies such as low-shear pelletizing, direct dosing of shredded material, or solvent-based recycling approaches could help reduce degradation at this stage.

Overall, the findings demonstrate that EPS bead foams maintain stable processing and consistent mechanical performance over multiple recycling cycles when blended with virgin material as prescribed by the PPWR. However, pelletizing conditions must be carefully controlled in future large-scale circular EPS processes to avoid the degradation observed in the C + 1 loop. If the EPS industry addresses the identified challenges in developing high quality recycled products, the already substantial recycling rates achieved in the EU for EPS packaging [23] will further increase in the next decade.

Author Contributions

Christian Töpfer: conceptualization, formal analysis, data curation, investigation, visualization, validation, writing – review and editing, writing – original draft. **Kristina Schüllner:** conceptualization, data curation, formal analysis, investigation, validation, visualization, writing – review and editing, writing – original draft. **Holger Ruckdäschel:** funding acquisition, project administration, supervision, writing – review and editing, validation.

Acknowledgments

The authors would like to thank Rika Scheider for performing the GPC measurements and for her valuable technical support. Furthermore, they would like to thank Max Löhner, who carried out the prefoaming and steam-based molding trials and Markus Schirmer, who conducted the extrusion trials. Open Access funding enabled and organized by Projekt DEAL.

Funding

The experimental study was funded by EUMEPS (European Manufacturers of Expanded Polystyrene). The sponsor had no influence on data analysis or interpretation of the results.

Data Availability Statement

The data that support the findings of this study are available from the corresponding author upon reasonable request.

References

1. P. R. Stupak, W. O. Frye, and J. A. Donovan, "The Effect of Bead Fusion on the Energy Absorption of Polystyrene Foam. Part I: Fracture

15482634, 2026, 3, Downloaded from https://4spepublications.onlinelibrary.wiley.com/doi/10.1002/pen.70290 by Universitaet Bayreuth, Wiley Online Library on [07/04/2026]. See the Terms and Conditions (https://onlinelibrary.wiley.com/terms-and-conditions) on Wiley Online Library for rules of use; OA articles are governed by the applicable Creative Commons License

Toughness," *Journal of Cellular Plastics* 27 (1991): 484–505, https://doi.org/10.1177/0021955X9102700503.

2. E. Velásquez, C. López-de-Dicastillo, A. Tapia, et al., "Repetitive Mechanical Recycling of Post-Consumer High Impact Polystyrene From Yogurt Cups: A Pilot-Scale Performance Assessment at Different Reprocessing Cycles," *Resources, Conservation and Recycling* 202 (2024): 107368, https://doi.org/10.1016/j.resconrec.2023.107368.

3. D. Raps, N. Hossieny, C. B. Park, and V. Altstädt, "Past and Present Developments in Polymer Bead Foams and Bead Foaming Technology," *Polymer* 56 (2015): 5–19, https://doi.org/10.1016/j.polymer.2014.10.078.

4. J. Rossacci and S. Shivkumar, "Bead Fusion in Polystyrene Foams," *Journal of Materials Science* 38 (2003): 201–206, https://doi.org/10.1023/A:1021180608531.

5. Z. Xu, D. Sun, J. Xu, R. Yang, J. D. Russell, and G. Liu, "Progress and Challenges in Polystyrene Recycling and Upcycling," *ChemSusChem* 17 (2024): e09447, https://doi.org/10.1002/cssc.202400474.

6. D. R. Tapia-Blácido, G. J. Aguilar, M. T. de Andrade, M. F. Rodrigues-Júnior, and F. C. Guareschi-Martins, "Trends and Challenges of Starch-Based Foams for Use as Food Packaging and Food Container," *Trends in Food Science and Technology* 119 (2022): 257–271, https://doi.org/10.1016/J.TIFS.2021.12.005.

7. R. Q. Albuquerque, F. Stephan, A. Pongratz, C. Brütting, K. Krause, and H. Ruckdäschel, "Recycling of Thermoplastics With Machine Learning: A Review," *Advanced Functional Materials* 17 (2025): 09447, https://doi.org/10.1002/adfm.202509447.

8. T. Maharana, Y. S. Negi, and B. Mohanty, "Review Article: Recycling of Polystyrene," *Polymer-Plastics Technology and Engineering* 46 (2007): 729–736, https://doi.org/10.1080/03602550701273963.

9. Z. Xu, F. Pan, M. Sun, et al., "Cascade Degradation and Upcycling of Polystyrene Waste to High-Value Chemicals," *Proceedings of the National Academy of Sciences of the United States of America* 119 (2022): 1–8, https://doi.org/10.1073/pnas.2203346119.

10. Z. Huang, M. Shanmugam, Z. Liu, et al., "Chemical Recycling of Polystyrene to Valuable Chemicals via Selective Acid-Catalyzed Aerobic Oxidation Under Visible Light," *Journal of the American Chemical Society* 144 (2022): 6532–6542, https://doi.org/10.1021/jacs.2c01410.

11. D. S. Achilias, I. Kanellopoulou, P. Megalokonomos, E. Antonakou, and A. A. Lappas, "Chemical Recycling of Polystyrene by Pyrolysis: Potential Use of the Liquid Product for the Reproduction of Polymer," *Macromolecular Materials and Engineering* 292 (2007): 923–934, https://doi.org/10.1002/mame.200700058.

12. J. J. Park, K. Park, J. S. Kim, et al., "Characterization of Styrene Recovery From the Pyrolysis of Waste Expandable Polystyrene," *Energy & Fuels* 17 (2003): 1576–1582, https://doi.org/10.1021/ef030102l.

13. C. Muhammad, J. A. Onwudili, and P. T. Williams, "Thermal Degradation of Real-World Waste Plastics and Simulated Mixed Plastics in a Two-Stage Pyrolysis–Catalysis Reactor for Fuel Production," *Energy & Fuels* 29 (2015): 2601–2609, https://doi.org/10.1021/ef502749h.

14. Y. Liu, J. Qian, and J. Wang, "Pyrolysis of Polystyrene Waste in a Fluidized-Bed Reactor to Obtain Styrene Monomer and Gasoline Fraction," *Fuel Processing Technology* 63 (2000): 45–55, https://doi.org/10.1016/S0378-3820(99)00066-1.

15. A. Karaduman, "Pyrolysis of Polystyrene Plastic Wastes With Some Organic Compounds for Enhancing Styrene Yield," *Energy Sources* 24 (2002): 667–674, https://doi.org/10.1080/00908310290086590.

16. R. Miandad, M. A. Barakat, A. S. Aburiazaiza, M. Rehan, I. M. I. Ismail, and A. S. Nizami, "Effect of Plastic Waste Types on Pyrolysis Liquid Oil," *International Biodeterioration & Biodegradation* 119 (2017): 239–252, https://doi.org/10.1016/J.IBIOD.2016.09.017.

17. M. R. Reed, E. R. Belden, N. K. Kazantzis, M. T. Timko, and B. Castro-Dominguez, "Thermodynamic and Economic Analysis of a Deployable and Scalable Process to Recover Monomer-Grade Styrene From Waste Polystyrene," *Chemical Engineering Journal* 492 (2024): 152079, https://doi.org/10.1016/j.cej.2024.152079.

18. I. Baertsoen, "Advanced Recycling Plant Closes Chain of Crisp Bag and Yoghurt Pots," 2024, Indaver Website, https://indaver.com/news/single/press-release-advanced-recycling-plant-closes-chain-of-crisp-bags-and-yoghurt-pots.

19. Agilyx ASA, "Agilyx Technology Produces On-Spec Product in Japan," 2024, https://www.agilyx.com/agilyx-technology-produces-on-spec-product-in-japan/.

20. A. Lamtai, S. Elkoun, M. Robert, F. Mighri, and C. Diez, "Mechanical Recycling of Thermoplastics: A Review of Key Issues," *Waste* 1 (2023): 860–883, https://doi.org/10.3390/waste1040050.

21. J. DeMarco, "GESA Report: Expanded Polystyrene Enviromental Profile," 2024, https://www.prweb.com/releases/gesa-report-72-nations-lead-global-recycling-momentum-for-unep-recognized-expanded-polystyrene-eps-transport-packaging-302313833.html.

22. Conversio Market & Strategy, "The EPS-Industry's Journey Towards Circularity—Progress Report," 2021, https://www.eumeps.eu/eumeps-newsroom/publications/conversio-study-on-the-eps-industrys-industry-to-sustainability.

23. G. Orveillon, E. Pierri, L. Egle, et al., *Scoping Possible Further EU-Wide End-of-Waste and By-Product Criteria* (European Commission. Joint Research Centre, 2022), https://doi.org/10.2760/067213.

24. United Nations, "United Nations Environment Programme—Plastic Pollution Science (Updated for the Fourth Session of the Intergovernmental Negotiating Committee), Otawa," 2024, https://wedocs.unep.org/handle/20.500.11822/45368?show=full.

25. M. Larrain, S. Van Passel, G. Thomassen, et al., "Techno-Economic Assessment of Mechanical Recycling of Challenging Post-Consumer Plastic Packaging Waste," *Resources, Conservation and Recycling* 170 (2021): 105607, https://doi.org/10.1016/j.resconrec.2021.105607.

26. A. P. Adam, J. V. R. V. Gonçalves, L. C. Robinson, L. C. Da Rosa, and E. L. Schneider, "Recycling and Mechanical Characterization of Polymer Blends Present in Printers," *Materials Research* 20 (2017): 202–208, https://doi.org/10.1590/1980-5373-mr-2016-1099.

27. F. Welle, "Recycling of Post-Consumer Polystyrene Packaging Waste Into New Food Packaging Applications—Part 2: Co-Extruded Functional Barriers," *Recycling* 8 (2023): 1–15, https://doi.org/10.3390/recycling8020039.

28. F. Belblidia, M. H. Gabr, J. F. T. Pittman, and A. Rajkumar, "Recycling High Impact Polystyrene: Material Properties and Reprocessing in a Circular Economy Business Model," *Progress in Rubber, Plastics and Recycling Technology* 39 (2023): 343–363, https://doi.org/10.1177/14777606231168653.

29. J. Momanyi, M. Herzog, and P. Muchiri, "Analysis of Thermomechanical Properties of Selected Class of Recycled Thermoplastic Materials Based on Their Applications," *Recycling* 4 (2019): 33, https://doi.org/10.3390/recycling4030033.

30. F. d. S. M. Teixeira, A. C. de C. Peres, and E. B. A. V. Pacheco, "Mechanical Recycling of Acrylonitrile-Butadiene-Styrene Copolymer and High Impact Polystyrene From Waste Electrical and Electronic Equipment to Comply With the Circular Economy," *Frontiers in Sustainability* 4 (2023): 1203457, https://doi.org/10.3389/frsus.2023.1203457.

31. J. C. Capricho, K. Prasad, N. Hameed, M. Nikzad, and N. Salim, "Upcycling Polystyrene," *Polymers* 14 (2022): 5010, https://doi.org/10.3390/polym14225010.

32. G. Madras, "Molecular Weight Effect on the Dynamics of Polystyrene Degradation," *Industrial & Engineering Chemistry Research* 36 (1997): 2019–2024, https://doi.org/10.1021/ie9607513.

33. L. A. Wall, S. Straus, and R. E. Florin, "Pyrolysis of Anionic and Thermally Prepared Polystyrenes," *Journal of Research of the National*

15482634, 2026, 3, Downloaded from https://4spublications.onlinelibrary.wiley.com/doi/10.1002/pen.70290 by Universitaet Bayreuth, Wiley Online Library on [07/04/2026]. See the Terms and Conditions (https://onlinelibrary.wiley.com/terms-and-conditions) on Wiley Online Library for rules of use; OA articles are governed by the applicable Creative Commons License

Bureau of Standards Section A: Physics and Chemistry 77 A (1973): 157–170, https://doi.org/10.6028/jres.077A.009.

34. G. G. Cameron, J. M. Meyer, and i. T. McWalter, "Thermal Degradation of Polystyrene: 3.A Reappraisal," *Macromolecules* 11, no. 4 (1978): 696–700, https://doi.org/10.1021/ma60064a016.

35. F. Vilaplana, A. Ribes-Greus, and S. Karlsson, "Degradation of Recycled High-Impact Polystyrene. Simulation by Reprocessing and Thermo-Oxidation," *Polymer Degradation and Stability* 91 (2006): 2163–2170, https://doi.org/10.1016/j.polymdegradstab.2006.01.007.

36. Z. O. G. Schyns and M. P. Shaver, "Mechanical Recycling of Packaging Plastics: A Review," *Macromolecular Rapid Communications* 42 (2021): 2000415, https://doi.org/10.1002/marc.202000415.

37. P. W. Springer, R. S. Brodkey, and R. E. Lynn, "The Effects of Extrusion on the Molecular and Rheological Properties of General-Purpose Polystyrene," *Polymer Engineering and Science* 15 (1975): 588–593, https://doi.org/10.1002/pen.760150805.

38. K. Arisawa and R. S. Porter, "The Degradation of Polystyrene During Extrusion," *Journal of Applied Polymer Science* 14 (1970): 879–896, https://doi.org/10.1002/app.1970.070140402.

39. C. Capone, L. Di Landro, F. Inzoli, M. Penco, and L. Sartore, "Thermal and Mechanical Degradation During Polymer Extrusion Processing," *Polymer Engineering and Science* 47 (2007): 1813–1819, https://doi.org/10.1002/pen.20882.

40. C. Remili, M. Kaci, A. Benhamida, S. Bruzaud, and Y. Grohens, "The Effects of Reprocessing Cycles on the Structure and Properties of Polystyrene/Cloisite15A Nanocomposites," *Polymer Degradation and Stability* 96 (2011): 1489–1496, https://doi.org/10.1016/j.polymdegradstab.2011.05.005.

41. F. Soriano, G. Morales, and R. D. de León, "Recycling of High Impact Polystyrene in Coextruded Sheet: Influence of the Number of Processing Cycles on the Microstructure and Macroscopic Properties," *Polymer Engineering and Science* 46 (2006): 1698–1705, https://doi.org/10.1002/pen.20652.

42. R. C. Santana and S. Manrich, "Studies on Thermo-Mechanical Properties of Post-Consumer High Impact Polystyrene in Five Reprocessing Steps," *Progress in Rubber, Plastics and Recycling Technology* 18 (2002): 99–110, https://doi.org/10.1177/147776060201800202.

43. Z. O. G. Schyns, A. D. Patel, and M. P. Shaver, "Understanding Poly(Ethylene Terephthalate) Degradation Using Gas-Mediated Simulated Recycling," *Resources, Conservation and Recycling* 198 (2023): 107170, https://doi.org/10.1016/j.resconrec.2023.107170.

44. A. Shyichuk, K. Piszczek, and J. Rokitnicka, "Recovery of Mechanical Properties of Aged Polystyrene After Reprocessing," *Polimery* 51 (2006): 382–385, https://doi.org/10.14314/polimery.2006.382.

45. European Parliament and Council, *Regulation on Packaging and Packaging Waste - EU Regulation 2025/40* (2024), http://data.europa.eu/eli/reg/2025/40/oj.

46. R. Q. Albuquerque, J. Meuchelböck, and H. Ruckdäschel, "A Unified Approach for Evaluating Mechanical Compression Tests for Polymer Bead Foams," *Journal of Polymer Science* 62 (2024): 1034–1043, https://doi.org/10.1002/pol.20230704.

47. L. J. Gibson and M. F. Ashby, "Cellular Solids," in *Cambridge Solid State Science Series*, 2nd ed. (Cambridge University Press, 1997).

48. D. J. Fossey and C. H. Smith, "Determination of the Diffusivity of n-Pentane in Polystyrene Bead Foam," *Journal of Applied Polymer Science* 17 (1973): 1749–1770, https://doi.org/10.1002/app.1973.070170609.

49. H. Hajova, J. Chmelar, A. Nistor, T. Gregor, and J. Kosek, "Experimental Study of Sorption and Diffusion of n-Pentane in Polystyrene," *Journal of Chemical and Engineering Data* 58 (2013): 851–865, https://doi.org/10.1021/je300916f.

50. R. Gendron and M. F. Champagne, "Effect of Physical Foaming Agents on the Viscosity of Various Polyolefin Resins," *Journal of Cellular Plastics* 40 (2004): 131–143, https://doi.org/10.1177/0021955X04041959.

51. D. Raps, *Structure-Property Relationships of Polystyrene-Based Bead Foams* (University Bayreuth, 2019), https://epub.uni-bayreuth.de/id/eprint/5200/.

52. H. M. da Costa, V. D. Ramos, and M. G. de Oliveira, "Degradation of Polypropylene (PP) During Multiple Extrusions: Thermal Analysis, Mechanical Properties and Analysis of Variance," *Polymer Testing* 26 (2007): 676–684, https://doi.org/10.1016/j.polymertesting.2007.04.003.

53. A. A. Costa, P. G. Martinho, and F. M. Barreiros, "Comparison Between the Mechanical Recycling Behaviour of Amorphous and Semicrystalline Polymers: A Case Study," *Recycling* 8 (2023): 12, https://doi.org/10.3390/recycling8010012.

54. S. G. Howell, "A Ten Year Review of Plastics Recycling," *Journal of Hazardous Materials* 29 (1992): 143–164, https://doi.org/10.1016/0304-3894(92)85066-A.

55. P. G. Andersen, M. Hoelzel, and T. Stirner, "Feed Enhancement Technology for Low Bulk Density Material Into Co-Rotating Twin-Screw Compounding Extruders," in *Society of Plastics Engineers—EUROTEC 2011 Conference Proceedings* (2011).

56. E. M. Kampouris, C. D. Papaspyrides, and C. N. Lekakou, "A Model Process for the Solvent Recycling of Polystyrene," *Polymer Engineering and Science* 28 (1988): 534–537, https://doi.org/10.1002/pen.760280808.

57. M. T. García, I. Gracia, G. Duque, A. de Lucas, and J. F. Rodríguez, "Study of the Solubility and Stability of Polystyrene Wastes in a Dissolution Recycling Process," *Waste Management* 29 (2009): 1814–1818, https://doi.org/10.1016/j.wasman.2009.01.001.

Supporting Information

Additional supporting information can be found online in the Supporting Information section. **Table S1:** pen70290-sup-0001-TableS1.docx.

15482634, 2026, 3, Downloaded from https://4spepublications.onlinelibrary.wiley.com/doi/10.1002/pen.70290 by Universitaet Bayreuth, Wiley Online Library on [07/04/2026]. See the Terms and Conditions (https://onlinelibrary.wiley.com/terms-and-conditions) on Wiley Online Library for rules of use; OA articles are governed by the applicable Creative Commons License